



35 years of x-ray reflectivity at NSLS: (1) science hiding in small features & (2) the new kid (instrument) on the block

Ben Ocko
NSLS II, Brookhaven National Lab

ORSO: June 14, 2021



Modern x-ray reflectivity story: starts with Jens Als-Nielsen & Peter Pershan



1985: Jens and Peter at the D4 beamline (Doris, HASYLAB) running Tascom software on a PDP-11. These were the earliest early days in the field with studies on liquid crystal and water surfaces.

Transition to solid surfaces, studies at X22B at NSLS

- 1985-1989

Harvard Graduate students in
Physics and Chemistry



Ian Tidswell, Physics
(business world)



Steve Wasserman,
Chemistry (long career in
protein crystallography)

- 1985: (Harvard U) while a post-doc with Peter Pershan and George Whitesides were interested in using XR to study Thiols on Au (deposited on Mica)?
- Difficult due to strong Au scattering.
- Chose to study silanes (OTS) monolayers on glass (actually SiO₂/Si), a system discovered by Jacob Sagiv (Weizmann Institute)
- Ellipsometry had been the tool of choice

Historical: Origin of the term self-assembly

20

New Scientist 7 April 1983

MONITOR

Monolayer films that assemble themselves

MONOLAYER films—layers of material just one molecule thick—have many potential uses, ranging from the construction of synthetic biological membranes to micro-electronic applications (see *New Scientist* vol 95, p 912). Now Lucy Netzer and Jacob Sagiv, from the Weizmann Institute of Science, Rehovot in Israel have developed a simpler and quicker technique for preparing monolayer films that relies simply on the chemical properties of the starting materials. In effect the molecules assemble themselves (*Journal of the American Chemical Society*, vol 105, p 674). So far, Netzer and Sagiv have made films up to three monolayers thick using the new method.

The standard technique for producing monolayer films was pioneered by Langmuir and Blodgett (LB) in the 1930s. It employs mechanical means to organise molecules into a monolayer on the surface of a liquid. This layer can be transferred onto the surface of another material by dipping the latter into the liquid. Repeated dipping will produce films many monolayers thick. The drawbacks of the LB procedure are that it is slow, not easily applied to large areas and doesn't always produce a film with the desired structure.

Scientists examining alternative

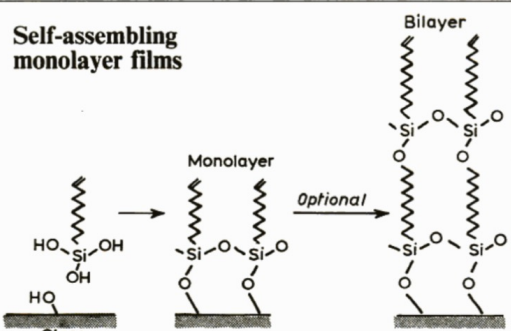
approaches are attracted to the idea of using molecules that are chemicals designed to assemble themselves into a film. Netzer and Sagiv designed a long chain molecule with a reactive chemical group at one end and an inert group at the

after one monolayer has formed. They tried their idea out on a piece of glass which they dipped into a solution containing their compound. Within two minutes a monolayer was produced. The reactive heads of the molecules could also react with one another, forming cross-links that made the film very strong. Chloroform, which easily dissolved the original compound, did not remove the monolayer.

To prepare multilayer films, the Israeli scientists first needed to modify their special molecule. They replaced the unreactive end with a new chemical group. Although this group is inert, it could be turned into an hydroxyl group at a later stage. The outer surface would then be covered with hydroxyl groups, like the original surface, and the process could be repeated.

By repeating this "activation" process twice, the researchers managed to make a film three monolayers thick. However, the second and third layers were 20-30 per cent less compact than the first.

These experiments demonstrate clearly that self-assembly is a feasible approach to monolayer formation. The design of the molecule predetermines the structure of the film and covering large areas should prove no problem—important advantages over the LB technique. □



The new technique uses molecules that can self-assemble—their reactive ends bonding with hydroxyl groups on the glass surface, and their unreactive ends sticking upwards. The monolayer can be activated to produce bi- and trilayers

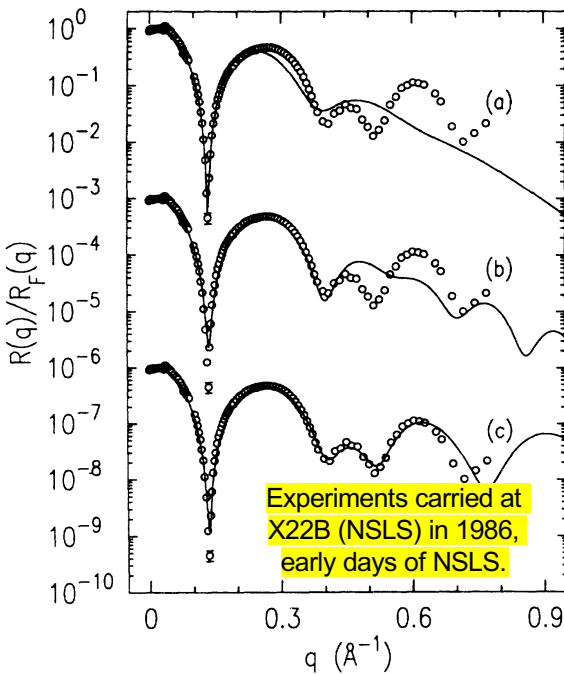
opposite end. They chose a reactive group that would bind to a solid surface with hydroxyl groups (-OH) sticking out. They hoped that the molecules would react with the surface to form a film, with the long chains all sticking out like a field of corn. Since the outermost ends of the molecules are unreactive the reaction should stop

New *Scientist* story in 1983 about the silane work of the Sagiv Group, predates Harvard groups work on thiols on Gold.

"Self-assembly" term was coined by the journal

Seminal XR Paper on Silane (OTS) monolayers on SiO₂/Si

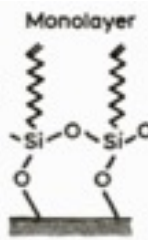
In-plane study shows that molecules are well-packed with 20.5 Å² /molecules



One-layer (small q)

One-layer (all q)

Three-layers (all q)



PHYSICAL REVIEW B

VOLUME 41, NUMBER 2

15 JANUARY 1990-I

X-ray specular reflection studies of silicon coated by organic monolayers (alkylsiloxanes)

I. M. Tidwell, B. M. Ocko,^a and P. S. Pershan

^aDivision of Applied Sciences and Department of Physics, Harvard University, Cambridge, Massachusetts 02138

S. R. Wasserman and G. M. Whitesides

Department of Chemistry, Harvard University, Cambridge, Massachusetts 02138

J. D. Axe

Department of Physics, Brookhaven National Laboratory, Upton, New York 11973

(Received 3 October 1988; revised manuscript received 7 August 1989)

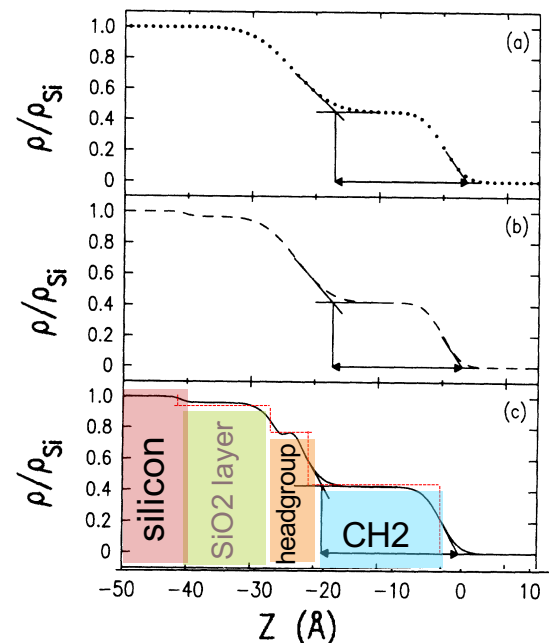
J. Am. Chem. Soc. 1989, 111, 5852–5861

The Structure of Self-Assembled Monolayers of Alkylsiloxanes on Silicon: A Comparison of Results from Ellipsometry and Low-Angle X-ray Reflectivity

Stephen R. Wasserman,^a George M. Whitesides,^{a,*†} Ian M. Tidwell,^b Ben M. Ocko,^b Peter S. Pershan,^{a,*‡} and John D. Axe^b

800 citations between these two papers

~ 2nm thick, chemically bonded monolayer, very stable

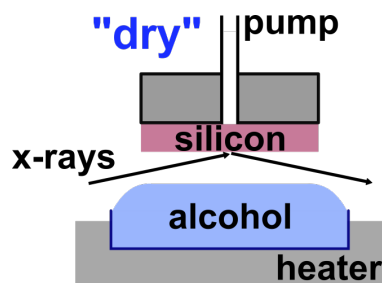
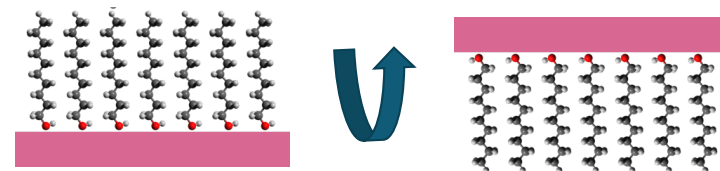


- Box model fits
- Three layers required
- Best fit parameters
- SiO₂ layer 13 Å ✓
- SiO₂ density 96% of Si ✓
- Head-group layer 7 Å ??
- CH₂ layer 21 Å ✓
- 21 Å/17CH₂ = 1.24 Å/CH₂ ✓
- CH₂ density 43% of Si
0.31 e/Å³ ✓

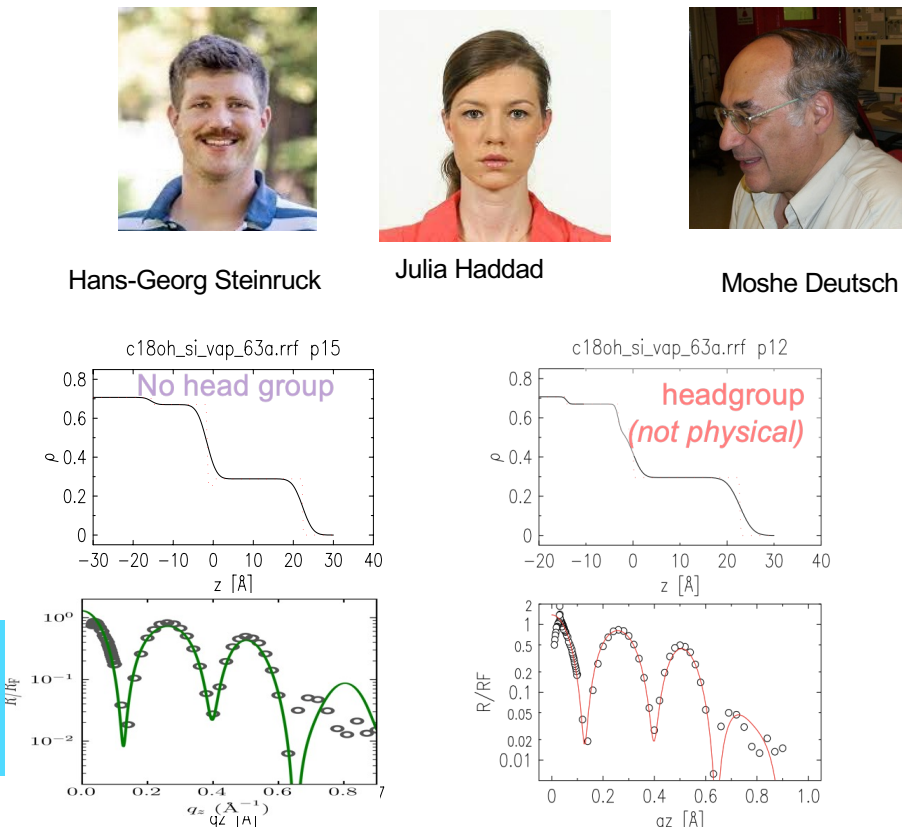
Why is the head-group layer so thick ??
Is this the correct model?

CCCCCCCCCCCCCCCCCO

C18OH monolayers on SiO₂/Si (native oxide)



- Also a C18 monolayer
- Hydrogen bonding.
- Data to larger q



Same SiO₂ model as 1989 OTS analysis
Used “successfully” in about 100 papers

Fails at large q!!
bad data or the wrong model?
Troubling for about a year



Hans-Georg Steinruck



Julia Haddad

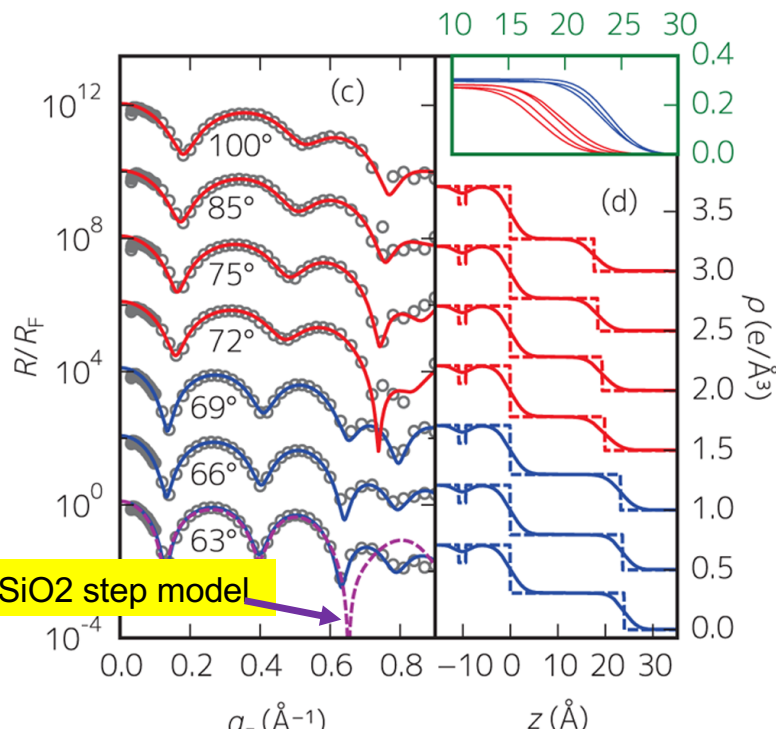


Moshe Deutsch



C₁₈OH monolayers on SiO₂/Si

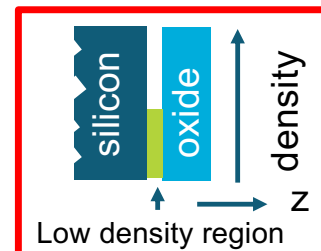
in equilibrium with its vapor (new oxide model required)



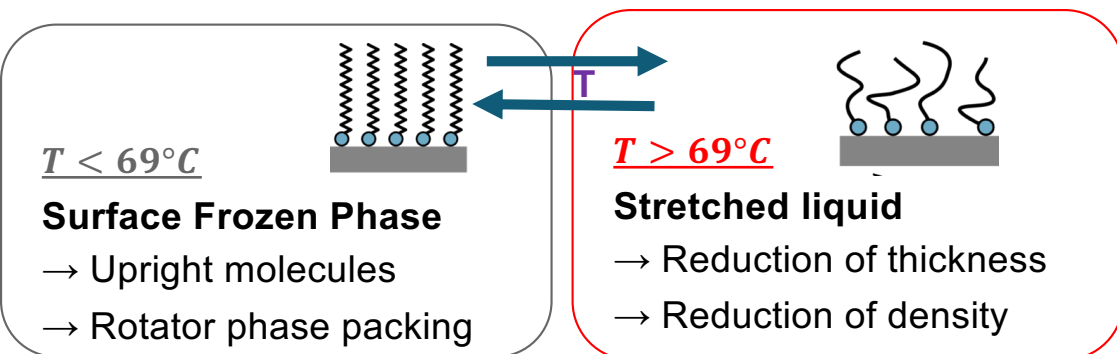
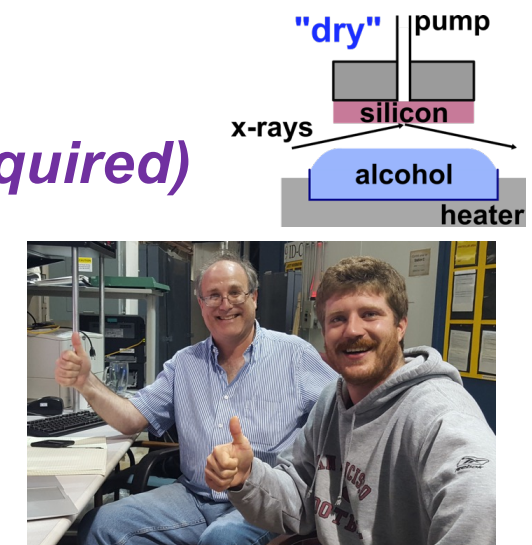
Brookhaven National Laboratory

Modelling:
3 layer model (dip, oxide, SAM)
Fit: Only SAM parameters

New oxide model

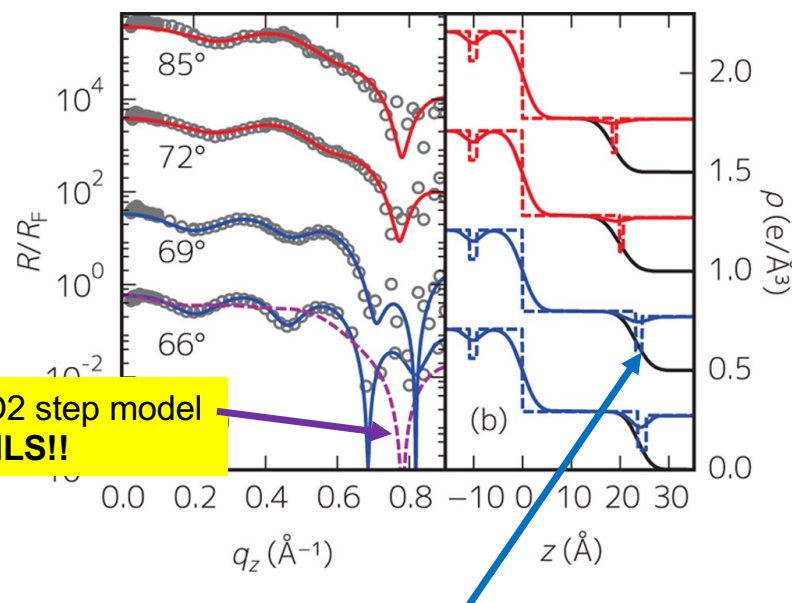


- SiO₂ layer 10 Å thick
- Density depletion between Si & SiO₂
- Same model works at all temperatures
- Perfect in frozen & stretched liquid states

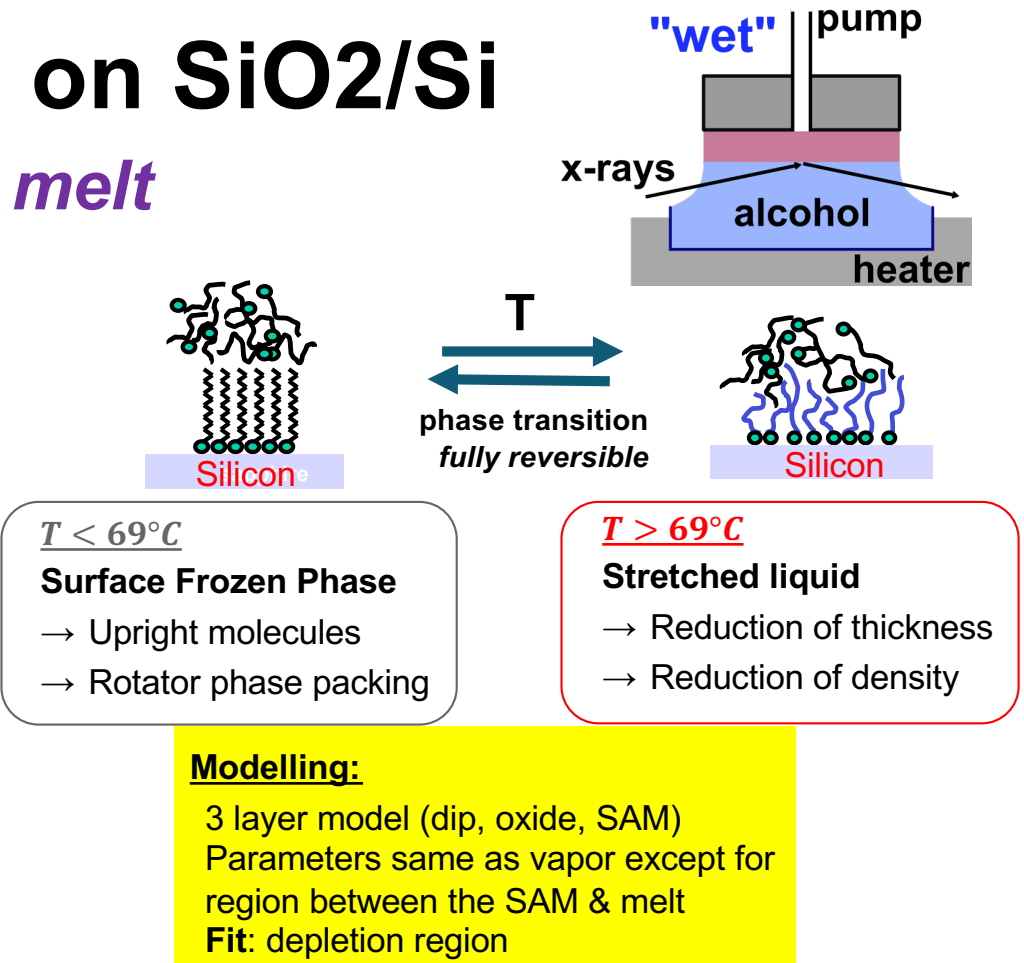


J Haddad, et al., JPCC 31, 17648 (2015)

C₁₈OH monolayers on SiO₂/Si in equilibrium with its melt



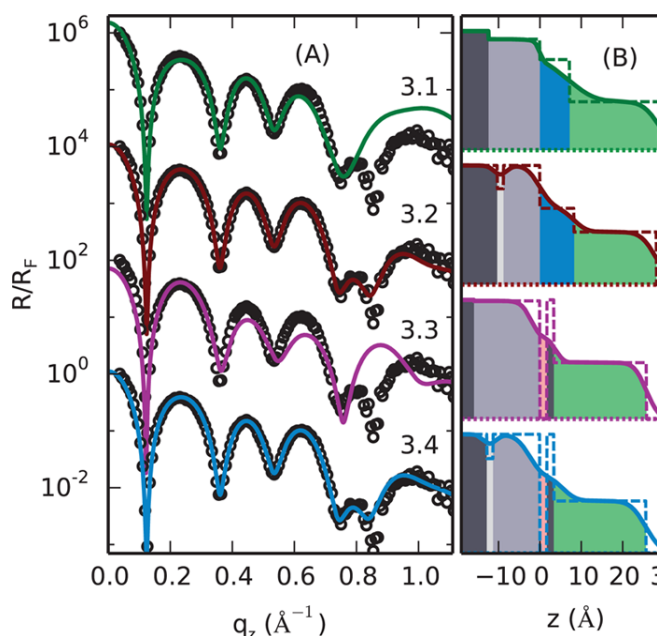
Contrast is from the density depletion region



Conclusion: Same density depletion oxide model works when in contact with the melt
→ increases confidence in the depletion oxide model

How does the improved oxide model work for OTS on SiO₂/Si?

Data to larger than 1989 study



HG=HeadGroup

- 1989 Si Step oxide
- 1989 Unphysical HG
- 2014 Si depletion oxide
- 1989 Unphysical HG
- 1989 Si Step oxide
- 2014 Realistic HG
- 2014 Si depletion oxide ✓
- 2014 Realistic HG ✓



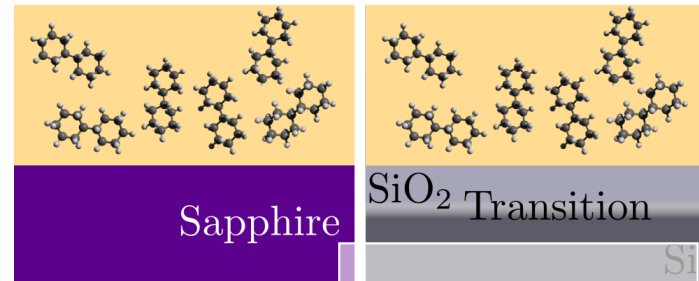
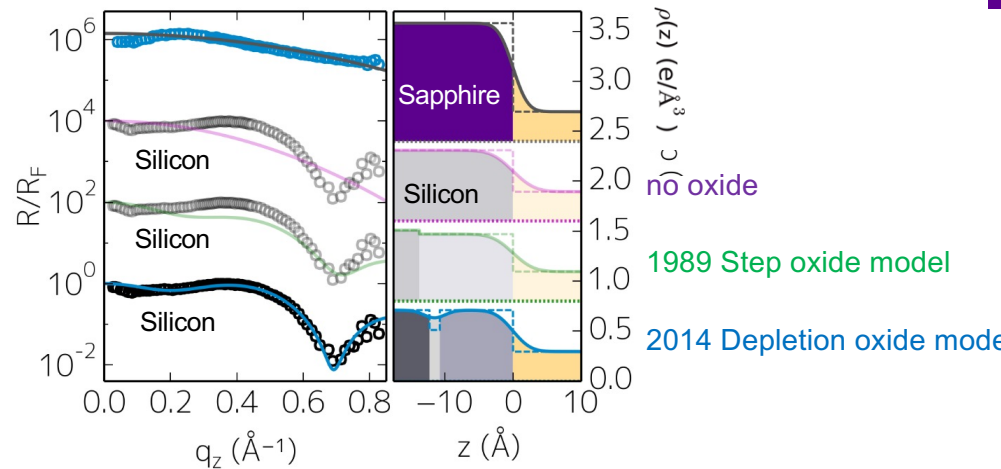
Hans-Georg Steinruck

- 3 slab model
- Oxide depletion (10 Å thick oxide)
- Physically motivated headgroup
- Model works for all chain length
- Fits work to much larger q than the step density oxide model

Conclusion: Further increase in confidence for the depletion oxide model

How else can we test the oxide model?

- Can not be tested on clean substrates in air
organics build up with time
- Can be tested at the liquid/solid interface
using bicyclohexyl (BCH) as the organic liquid



Depletion oxide model fits
XR with simple liquid at the
interface

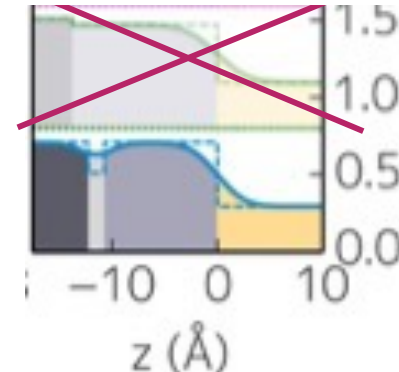


Conclusion: provides additional
confidence in the depletion oxide model

Native Silicon Oxide Summary

Significant since Silicon wafers are used for lots of XR and NR studies

✗ 1989 step oxide model
✓ 2014 depletion oxide model



Experimental Evidence

Depletion Si oxide model works well for

1. OTS on SiO₂/Si[1]
2. C₁₈OH on SiO₂/Si (vapor & liquid)[2]
3. Simple liquids[3]

Three times is the charm!!
(new oxide model replaces well cited 1989 model)

[1] H..G. Steinruck *et al.*, Langmuir 31, 11774-11780 (2015)

[2] J Haddad, *et al.*, JPCC 31, 17648 (2015)

[3] H.G. Steinruck et al., ACS Nano 12, 12676 (2014)

Physical motivation

- Si and SiO₂: Bond density mismatch
- Various oxidation states [4]
 - Dangling bonds, hydrogen
- Theory: Low density region [5]
- ~ 6 – 8 missing e⁻ per unit cell area
- Not sensitive to depletion thickness

[4] Braun *et al.*, Surf. Sci **180**, 279 (1987).

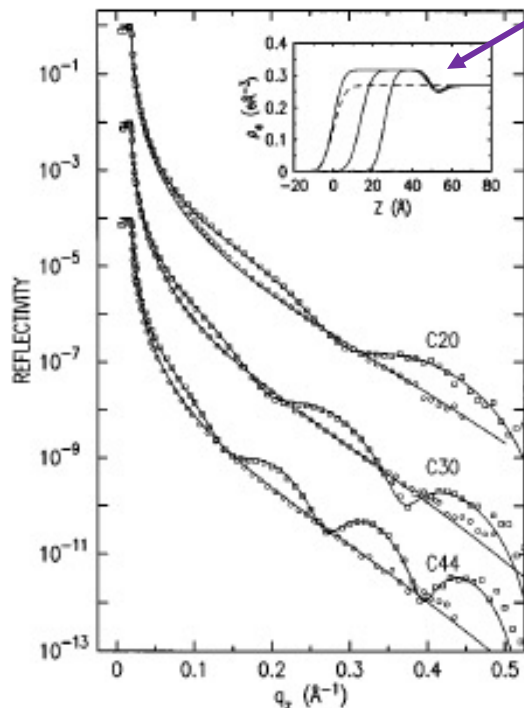
[5] Tu *et al.*, PRL **84**, 4393 (2000).

Surface Freezing

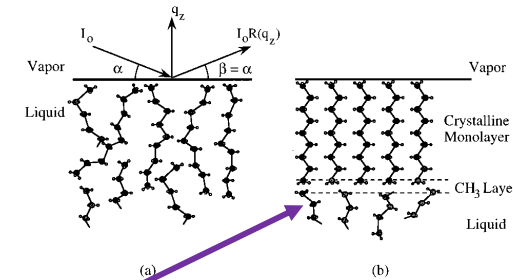
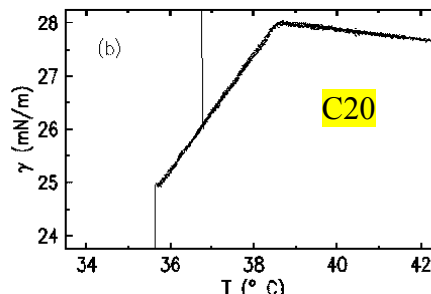
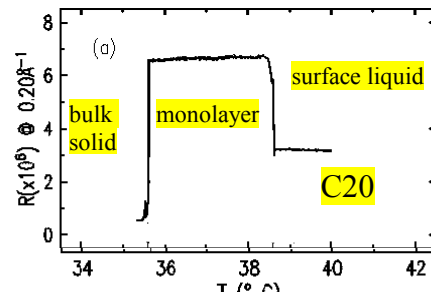
simple alkanes (vapor interface)



How does XR at a single q change with temperature?

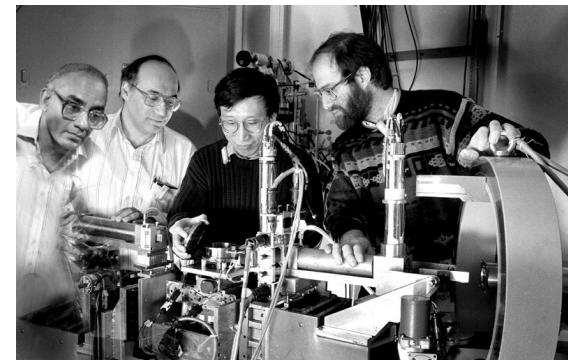


Small density depletion
CH₃ groups less dense



Formation of a single layer

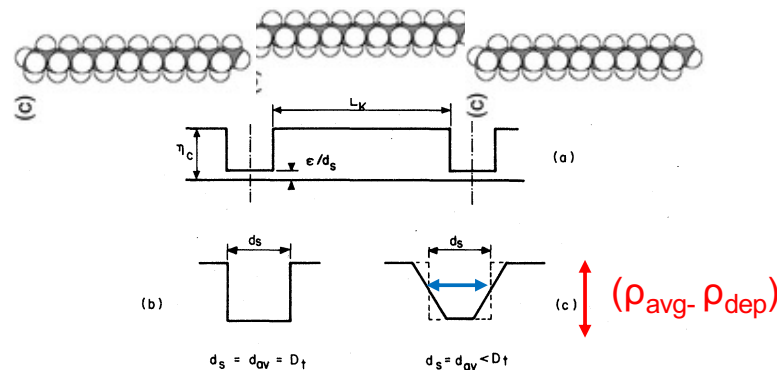
Agrees with the temperature range from surface tension measurements



X. Z. Wu, E. B. Sirota, S. K. Sinha, B. M. Ocko, and M. Deutsch, PRL 70, 958 (1993)

Methyl Region Depletion (alkanes and lipids)

Bulk Rotator Alkane Phases (Doucet)



Lipid Bilayers (Nagle)

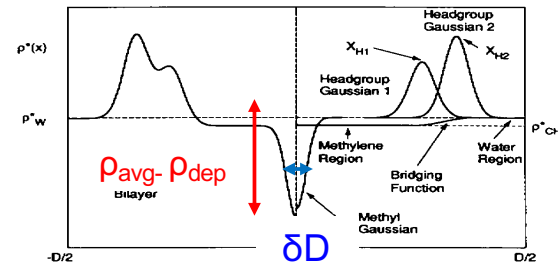


FIGURE I Electron density profile $\rho^*(x)$ as a function of distance x from the center of the bilayer for a 2G hybrid model is depicted on the left-hand side for half a bilayer. The right side depicts the constituent parts of the profile.

TABLE I. δD , ρ_{dep} , ρ_{avg} , and Γ as defined in the text.

System or interface	δD (\AA)	ρ_{dep} ($e\text{\AA}^{-3}$)	ρ_{avg} ($e\text{\AA}^{-3}$)	Γ ($e\text{\AA}^{-2}$)
Bulk alkane [6]	2.16	0.047	0.317	0.58
Lipid [7]	4.25	0.185	0.317	0.56

Measure of the integrated depletion

$$\Gamma = \delta D \times (\rho_{avg} - \rho_{dep})$$

Good agreement with
alkanes
lipids
frozen SAM monolayers (C18OH/SiO₂/Si)

Electron Depletion at SAM/liquid interface

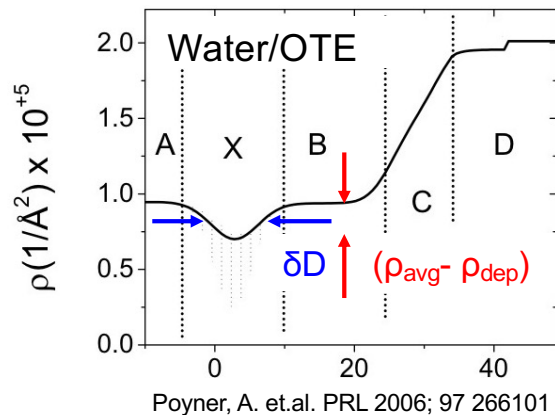
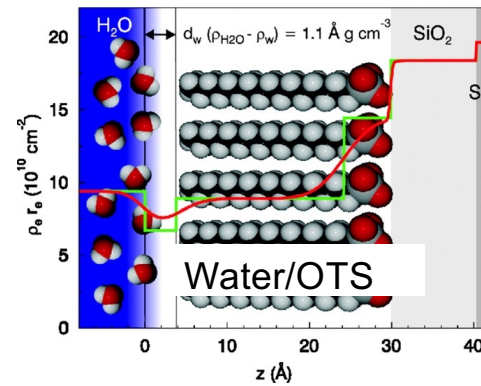


TABLE I. δD , ρ_{dep} , ρ_{avg} , and Γ as defined in the text.

System or interface	δD (\AA)	ρ_{dep} ($e\text{\AA}^{-3}$)	ρ_{avg} ($e\text{\AA}^{-3}$)	Γ ($e\text{\AA}^{-2}$)
Bulk alkane [6]	2.16	0.047	0.317	0.58
Lipid [7]	4.25	0.185	0.317	0.56
Water/OTE [4] (min)	1.8	0	0.334	0.60
Water/OTE [4] (max)	3.25	0	0.334	1.08
Water/OTS [5]	3.8	0.236	0.326	0.34

Electron Depletion always occur because of the low electron density methyl terminal groups



Mezger M. et.al. PNAS 2006;103:18401-18404

Ocko. Dhinojwala, Dallant, A.
et.al. PRL 2008; 101 039601

$$\Gamma = \delta D \times (\rho_{\text{avg}} - \rho_{\text{dep}})$$

Effective # of depleted carbon atoms

~1 missing carbon atoms"

CH3 volume nearly twice that of a CH2

Conclusion: Electron depletion at SAM water interface is not water depletion, primarily from the bulky methyl groups

Nanoscale Structure of the Oil-Water Interface

Scientific Achievement

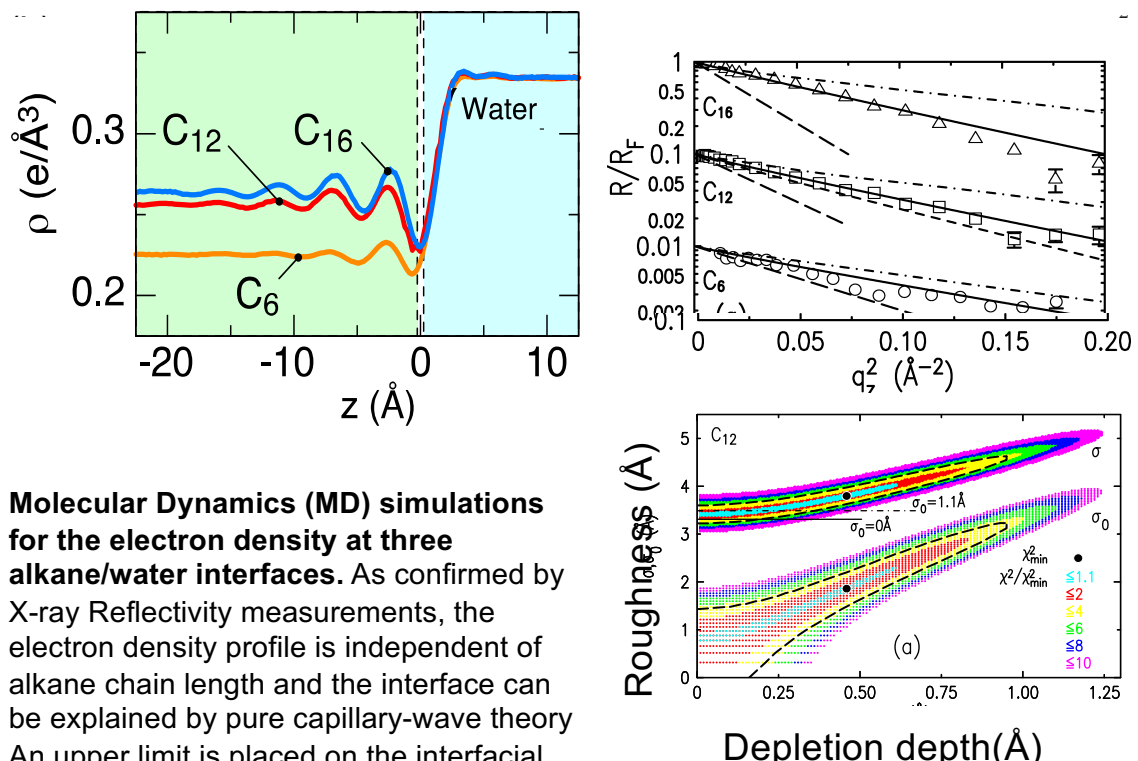
X-ray reflectivity (XR) and molecular dynamics (MD) simulations confirm that the nanoscale structure of liquid alkane-water interfaces can be explained by capillary wave theory with a very small depletion layer.

No preferential ordering of CH₃ units

Significance and Impact

Understanding alkane-water interfaces, the simplest hydrophobic-hydrophilic interfaces, is of fundamental importance.

M. Fukuto, B. M. Ocko, D. J. Bonthuis, R. R. Netz, H.-G. Steinrück, D. Pontoni, I. Kuzmenko, J. Haddad, M. Deutsch, *Physical Review Letters* 107, 256102 (2016)

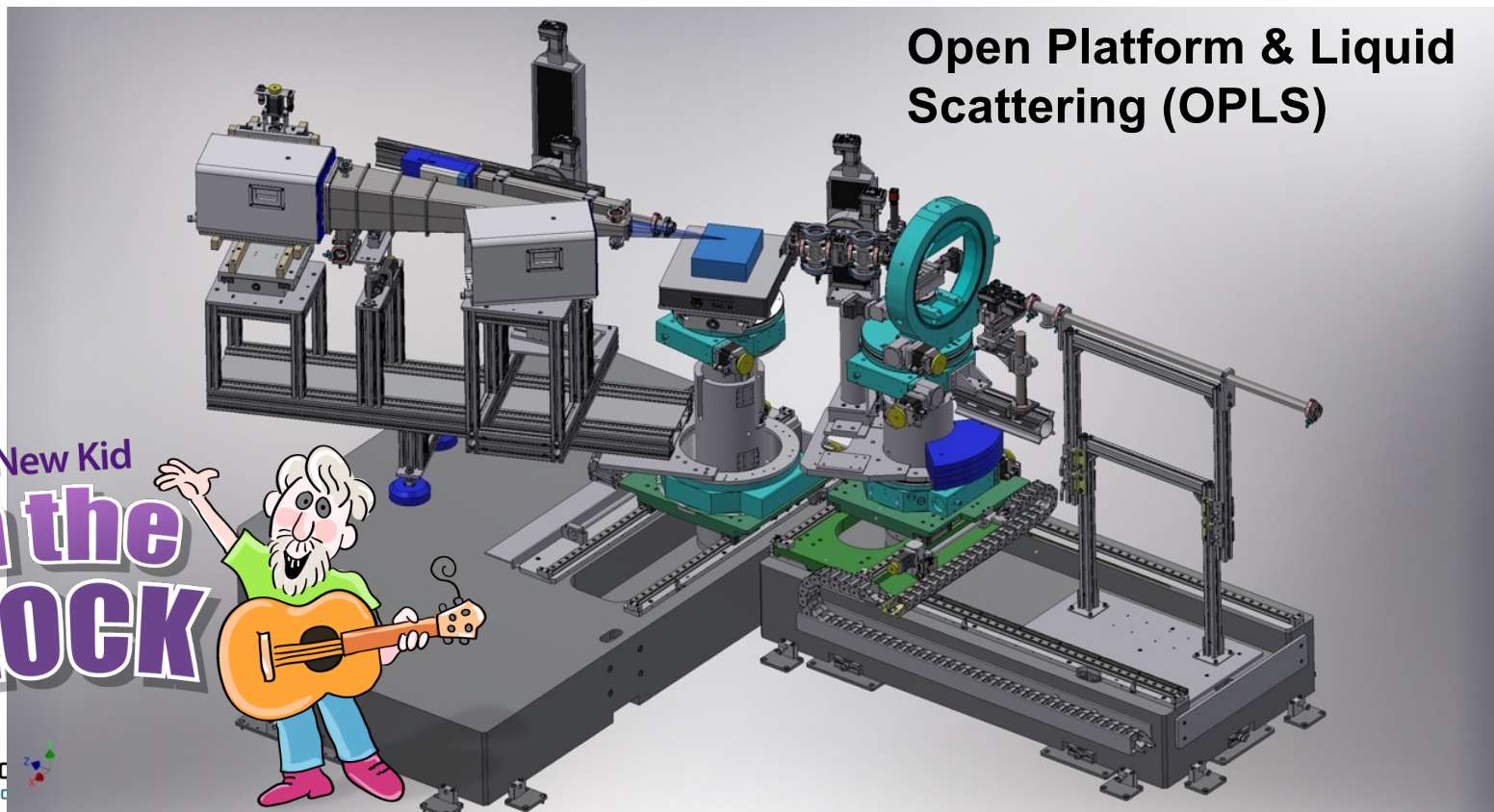


Molecular Dynamics (MD) simulations for the electron density at three alkane/water interfaces. As confirmed by X-ray Reflectivity measurements, the electron density profile is independent of alkane chain length and the interface can be explained by pure capillary-wave theory. An upper limit is placed on the interfacial depletion layer (dashed lines)

Fitting: Adding a depletion depth increases roughness more than CWM, *not physical*



Part 2: Recently commissioned liquids interface instrument at NSLS II



OPLS Instrument Perspective

Open Platform & Liquid Surfaces

World class instrument:

Beam shared with SMI SAXS-WAXS

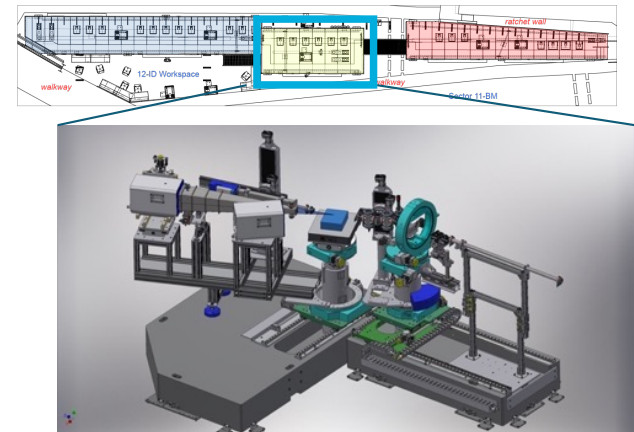
Open platform design for high versatility

Recycle existing hardware

Single crystal deflector design

capable 2-crystal deflector upgrade

Limitation: must fit in existing hutch with nearby wall



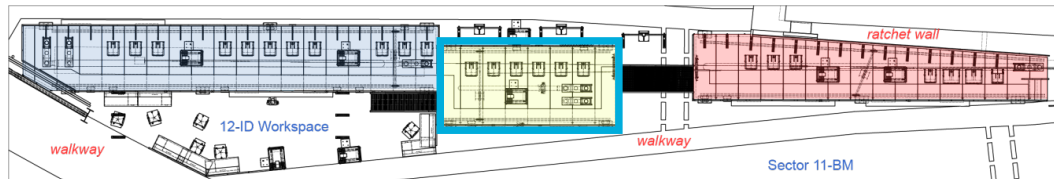
Methods: x-ray reflectivity, grazing angle fluorescence, grazing incident small & large angle incident scattering

Liquids sample environments/conditions: Langmuir troughs, liquid metals UHV chambers, small liquid/liquid and liquid vapor chambers, low vibrations (both passive and active), appropriate ventilation, sample weights up to 200 kg

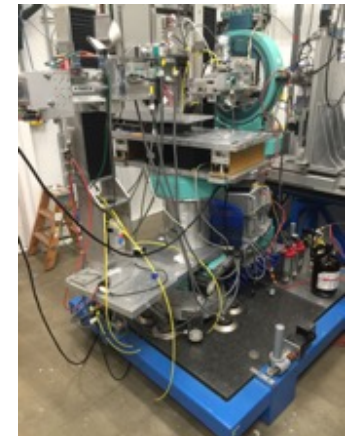
Processing sample environments/conditions: Roll-to-Roll Processing, additive manufacturing, vapor phase deposition: require complementary characterization.

Beam characteristics: ~10 µm vertical, 8-24 keV, high intensity, $\sim 10^{12}/\text{sec}$

NSLS Liquid Surfaces Historical Context



OPLS hutch



ANL/APS/CMC (9ID)
Liquid Spectrometer
1999-2015

1986-2014: Long history at BNL, liquid surface x-ray science pioneered at X22B, with Prof Peter Pershan, many seminal papers with Moshe Deutsch.

2011: SMI NEXT Project (shared beamline) approved. Includes liquids surface instrument in front hutch. SMI plan incorporated a double crystal deflector. liquid surface aspects curtailed in 2015. Hutch completed.

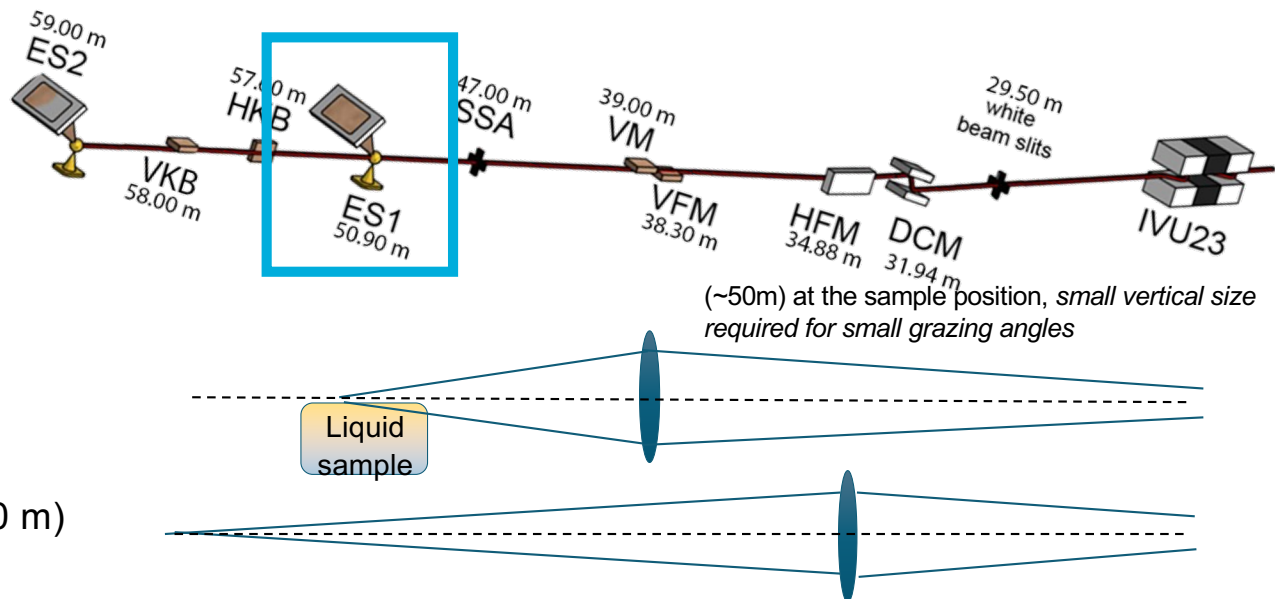
2016: PLS canted proposal: Expanded scope to include processing. Approved, not funded. *Mark Schlossman* played key role. **Canted beamline remains part of the long term NSLS II vision.** Start date is uncertain.

2017-2021: OPLS development project at SMI, shares beam time using existing front hutch completed with SMI project. Enhanced equipment from shuttered beamlines (APS/9ID) used. **Covid has been a challenge.**

2021: OPLS enters General User Operations



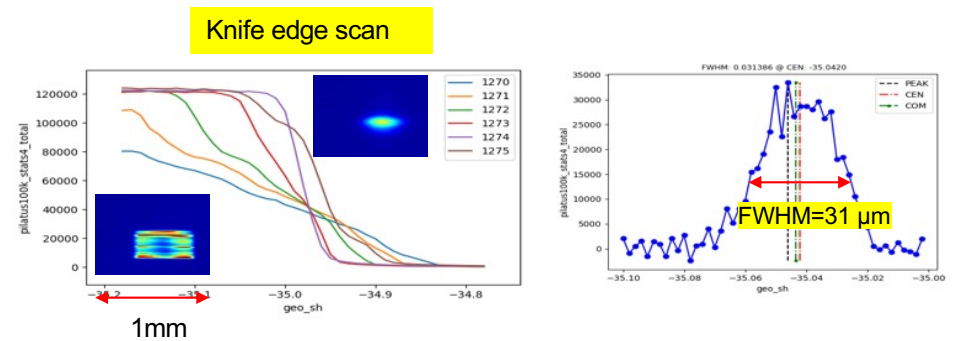
SMI optics



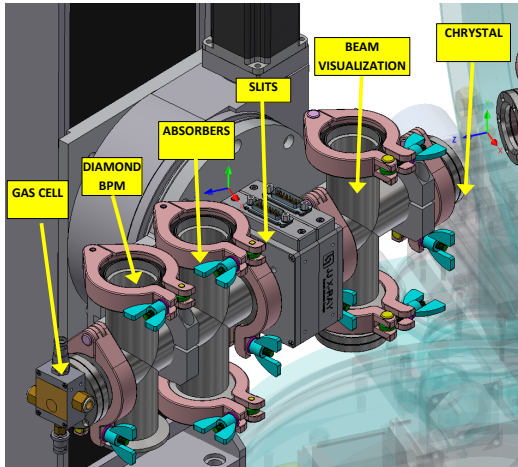
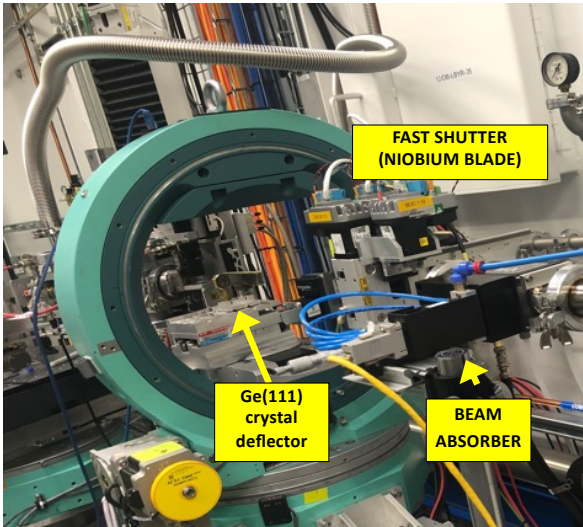
Vertical focus In ES1

Horizontal focus In ES2 (~60 m)

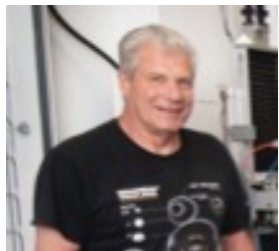
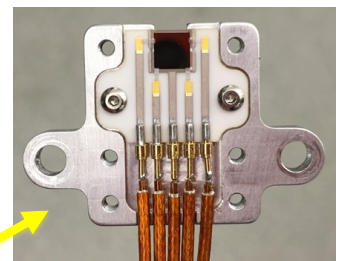
- Predicted optics, 14 μm FWHM vertical, measurement x2
- Bimorphs have imperfections or not ideally calibrated (room for improvement)



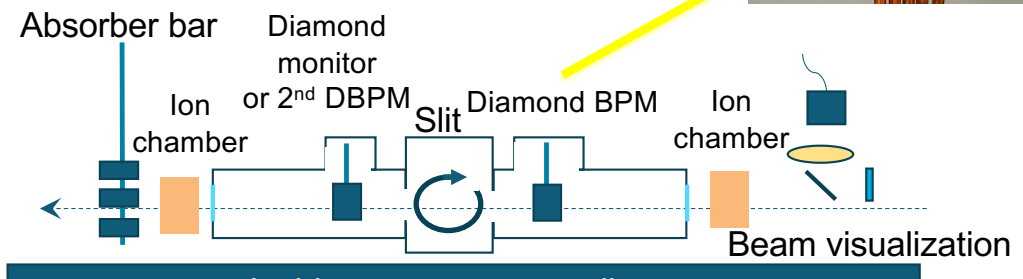
Crystal Deflector, Incident Flight Path & Diagnostics



Diamond Beam Position Monitor (DBPM)

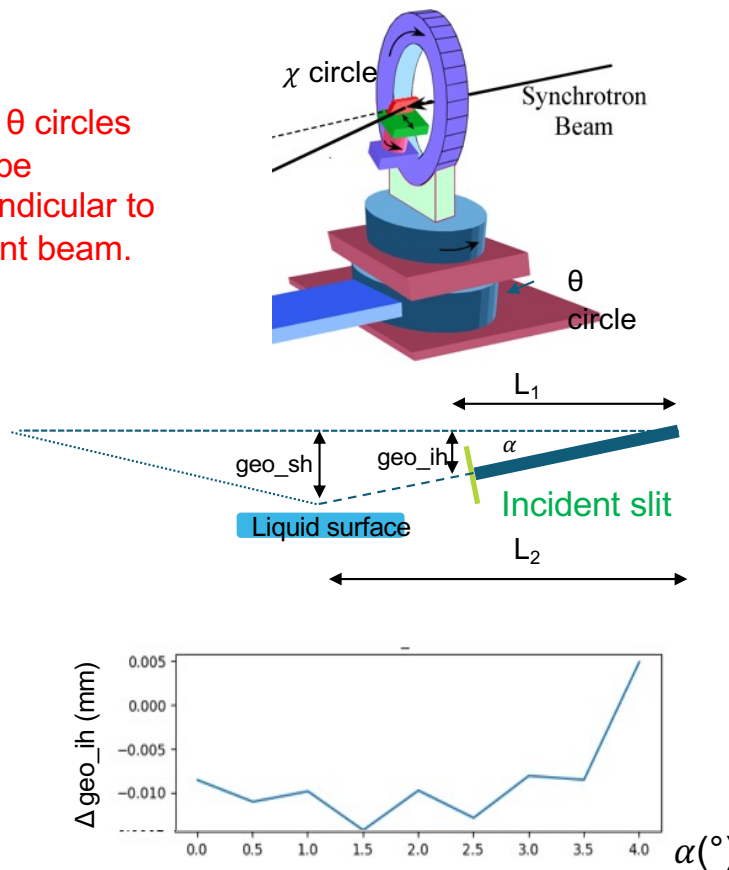


Rick Greene (master tech.)



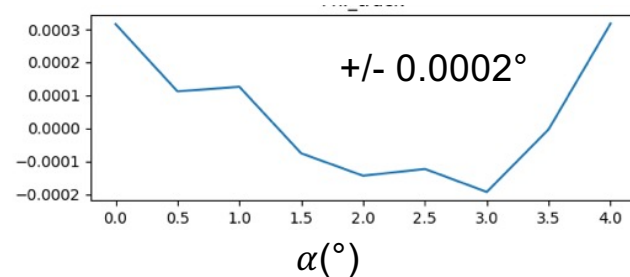
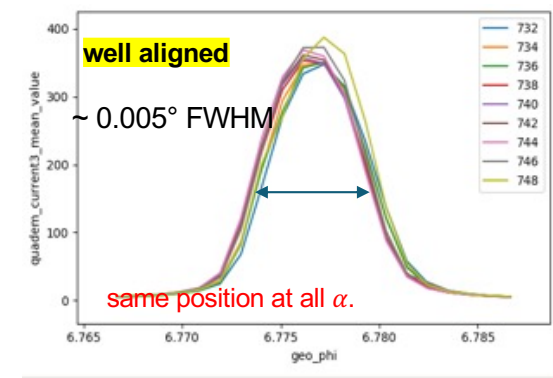
Instrument Tracking at 16.1keV

χ and θ circles
must be
perpendicular to
incident beam.



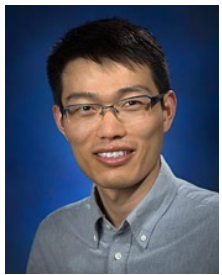
Plot shows +/- 2μm over range of interest (100ppm)
much smaller than the beam (meets spec)

Deflection crystal rocking
curves for $0^\circ < \alpha < 4^\circ$



Tracking errors are ~10% of rocking curve FWHM
Confirms Huber circles meet specifications

Commissioning- Water Reflectivity, variable trough sizes



Honghu Zhang
CFN Post-doc

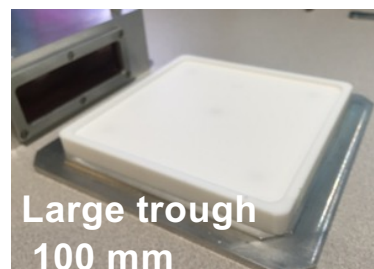
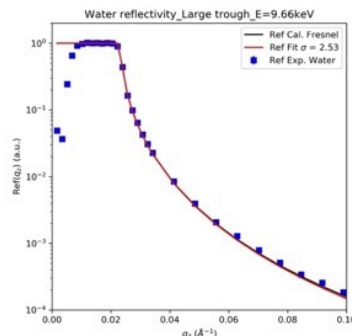


Guillaume
Freychet (SMI
scientist)

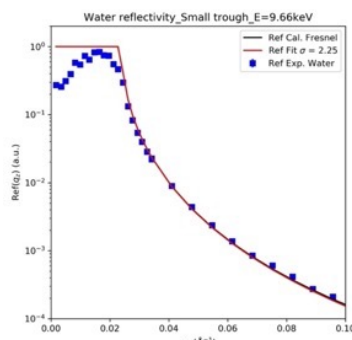


Maria Torres Arango
(CMS/SMI scientist)

E = 9.66keV

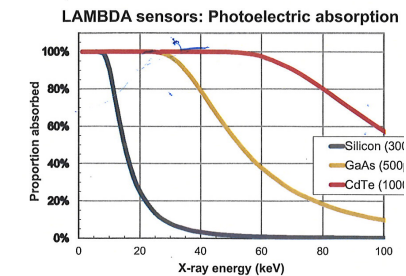


LAMBDA 250K,
GaAS



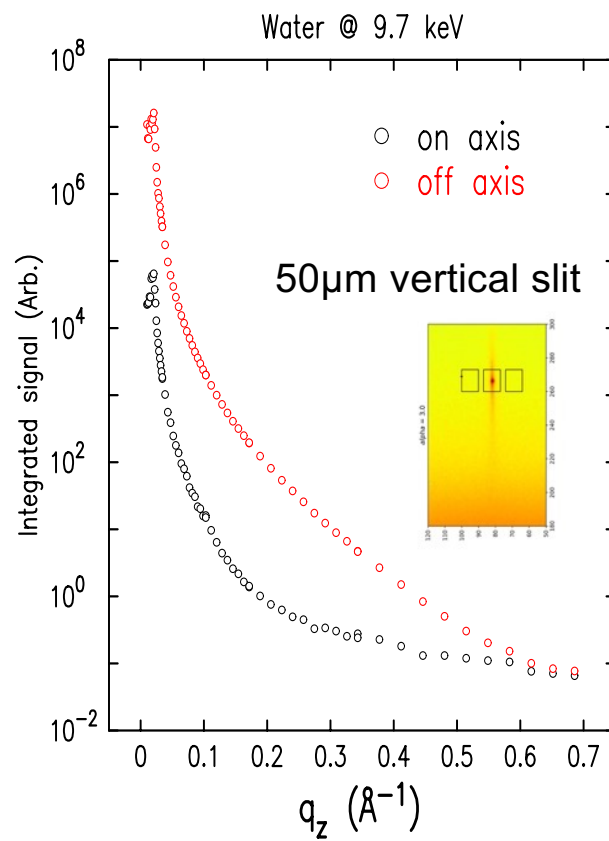
More precise tracking
required for smaller samples

~35 mm, Required for
expensive samples

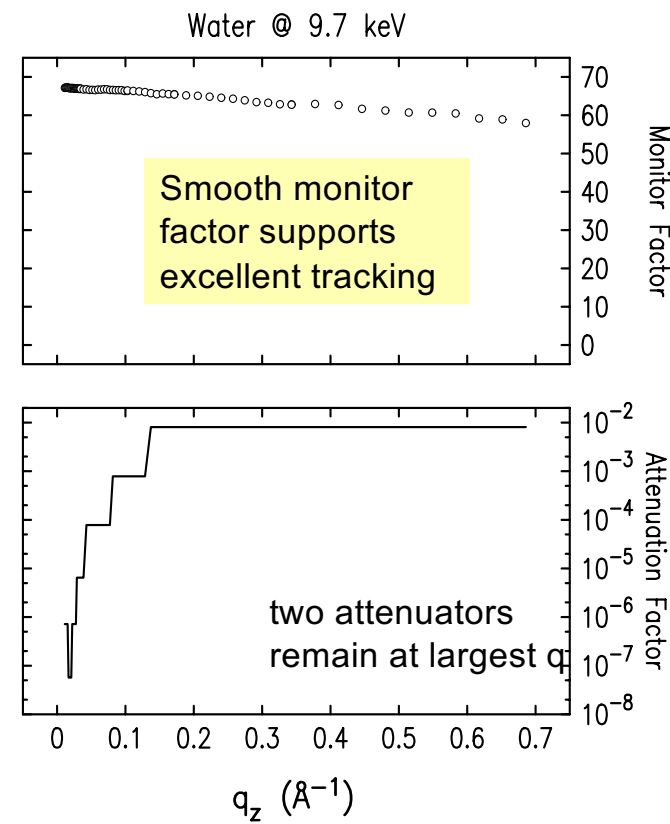


Water Reflectivity (automatic attenuation)

Each attenuator is ~ 10

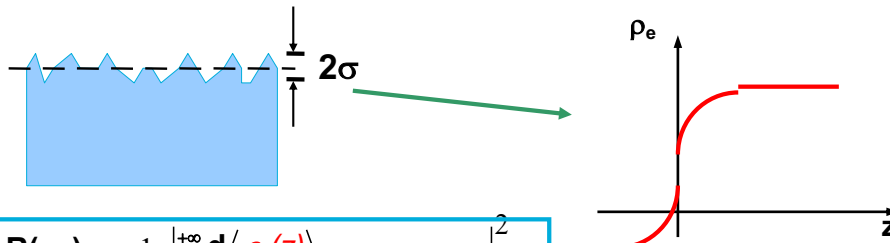


Large trough 100 mm

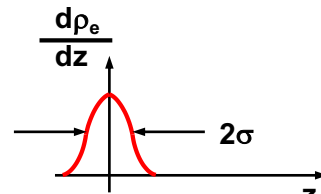


Do we still get the correct water capillary wave roughness physics after 35 yrs? YES

Capillary
wave
roughness



$$\frac{R(q_z)}{R_F(q_z)} = \frac{1}{\rho_\infty^2} \left| \int_{-\infty}^{+\infty} \frac{d\langle \rho_e(z) \rangle}{dz} \exp(iq_z z) dz \right|^2$$

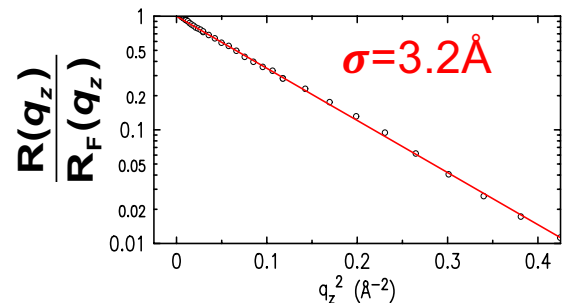
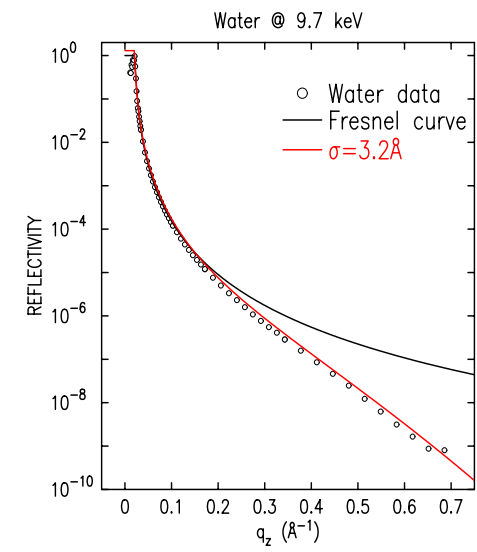


$$\frac{R(q_z)}{R_F(q_z)} = \exp(-q_z^2 \sigma^2)$$

$$\begin{aligned} \sigma^2(Q_z) &= \frac{\eta}{Q_z^2} \ln \left(\frac{\Delta Q_{xy}^{res}}{Q_{max}} \right) = \frac{k_B T}{2\pi\gamma} \ln \left(\frac{\Delta Q_{xy}^{res}}{Q_{max}} \right) \quad \text{Where } \eta = \frac{k_B T}{2\pi\gamma} Q_z^2 \\ &\equiv \left\langle \left(h(r_{xy}) - h(0) \right)^2 \right\rangle_{r_{xy}=\pi/\Delta Q_{xy}^{res}} \end{aligned}$$

Roughness depends on surface tension,
temperature, and resolution.

A. Braslau et al., *Phys. Rev. Lett.* (1985)

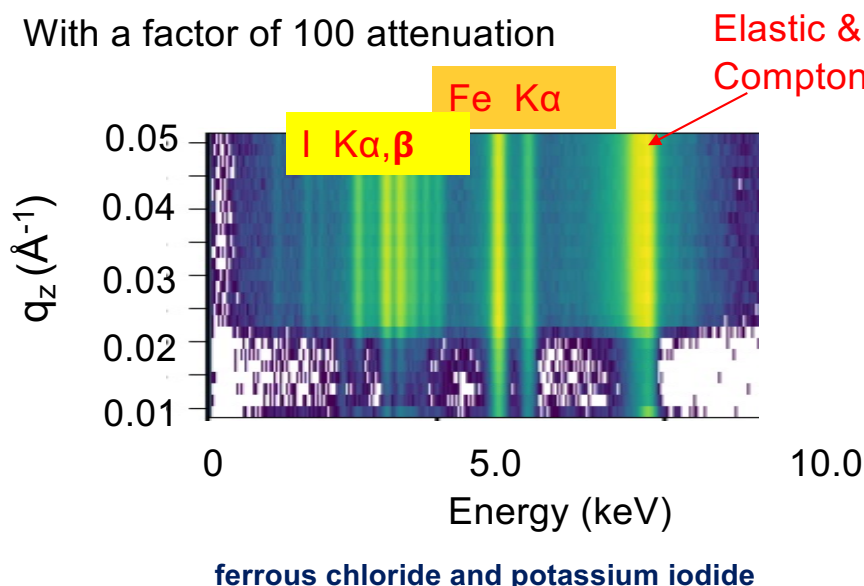


OPLS has entered General User Operations

mostly science commissioning

- ~30% of the SMI beamtime, shared with the SWAXS station.
- Summer 2021 cycle
 - 4 Science commissioning proposals were assigned time*
 - 4 other proposals already in the system (some will get fall time)*
 - Remote operations, few onsite users and staffing are challenging*
- Working Langmuir Trough expected in the fall
- PLS independent and canted (100%): **Remains part of the long term NSLS II vision**. Start date uncertain.
- **Over subscription is helpful. Contact me if you are considering applying for beamtime.**

Grazing Incident Angle X-ray Fluorescence (9.7 keV)



	K α_1	K α_2	K β_1
26 Fe	6,403.84	6,390.84	7,057.98
	L α_1	L α_2	L β_1
53 I	3,937.65	3,926.04	4,220.72
			4,507.5

Hitachi Vortex

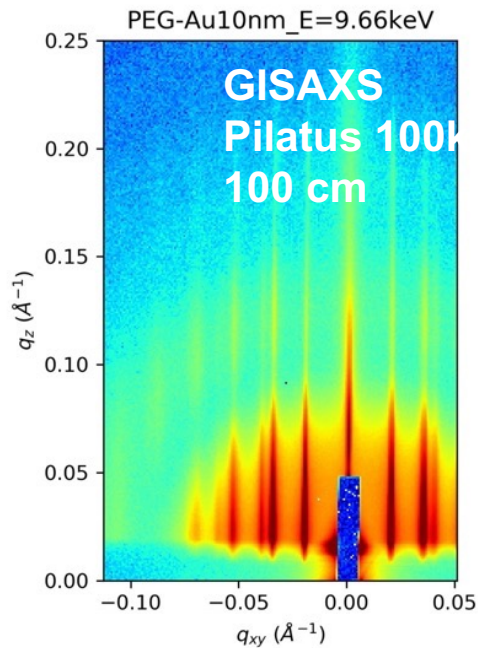


Express 3 mini

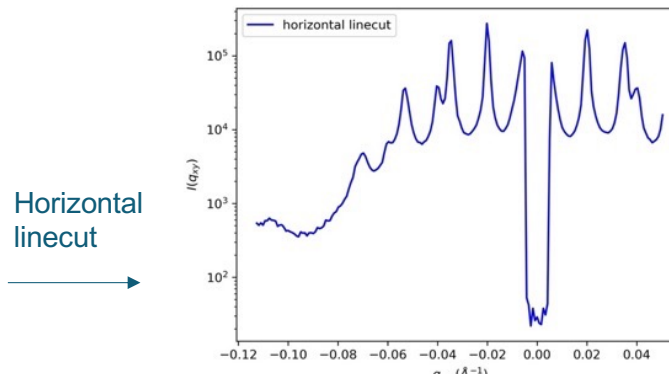
- Detector fits in slot (cell cover)
- Stays fixed when cell is translated
- 2 cm from the sample

- Should easily observe 2 keV(Cl) XRF
- Need to try with surfactants, calibration

GISAXS at OPLS: PEG-AuNPs (Vaknin Group)



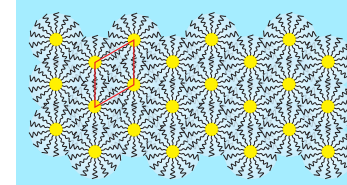
Incident angle $0.1^\circ = 0.785 \alpha_c$
Exposure time 0.1s
Pilatus 100k



$Q_i/Q_1 \approx 1 : \sqrt{3} : \sqrt{4} : \sqrt{7} : \sqrt{9} \dots$
Indicates hexagonal structure

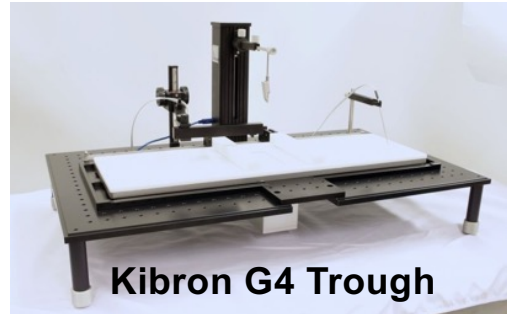
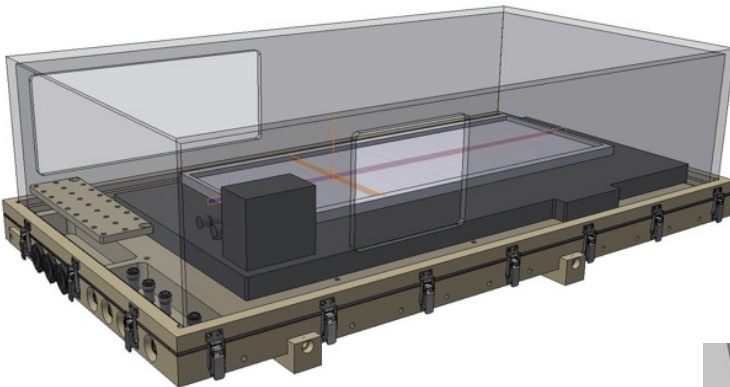
$$Q_1 = 0.020 \text{ \AA}^{-1}$$
$$d = 4\pi/Q_1/\sqrt{3} = 36.3$$

(b) nm hexagonal Superlattice

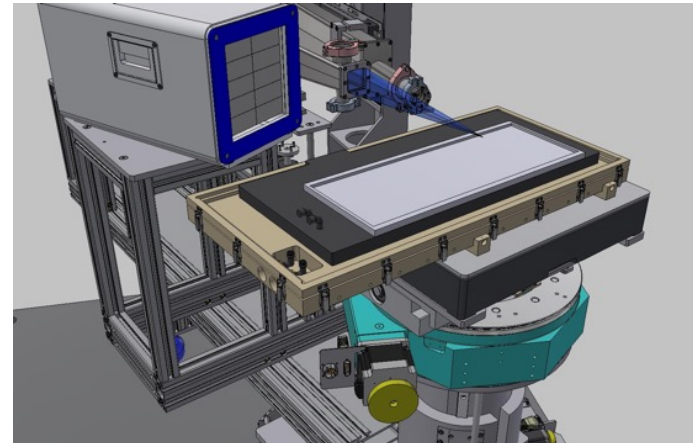


Follows results from H Zhang et al. Nanoscale (2017); JPCC (2017)

Modified Kibron G4 Langmuir Trough



- Modified Kibron G4 Trough (arrived).
- Single or double barrier modes
- All connections are through the base
- Cover can lift off and will be easy to redesign
- Enclosure is in the design phase.
- Helpful advice from Chen Shen (DESY)



Full BNL OPLS Team + outside reviews

Andrew Ackerman
Guillermo Aparicio
Barrett Clay
Daniel Bacescu
Michael Bebon
Lonny Berman
Mo Benmerrouche
Steve Bennett
Michael Bennett
Jimmy Biancarosa
Michael Bromfield
Scott Buda
Yong Cai
Stuart Campbell
Ed Cheswick
Sunil Chitra
Scott Coburn
Sandro Cunsolo

Guillaume Freychet
Masa Fukuto
George Ganetis
Kaz Gofron
Ed Granger
Rick Green
Brian Heneveld
Rodger Hubbard
Erik Johnson
Jeff Keister
Bob Lee
Bruce Lein
Ruipeng Li
Kenneth Evans-Lutterodt
Mike Maklary
Nikolay Malitsky
Jerry Malley
Thomas McDonald

Maxim Rakatin
Leo Reffi
Kristen Rubino
Andrew Sauerwald
Steve Sauter
Steve Sherwood
Richard Skelaney
Jean Smiles
Lori Stiegler
Jean Jordan-Sweet
Yuke Tian
Rob Todd
Maria Torres Arango
Andrew Walter
Lutz Wiegart
Benjamin Yavitt
Chenghao Yu
Honghu Zhang